

A Low-Cost Patch-Antenna for Non-Invasive Brain Cell Detection



Abdullah Alzahrani

Abstract: Cancer is one of the most frequent causes of death around the world. Brain tumour is a critical and dangerous type and have a few difficulties with the techniques used for their detection; it is hard to determine their location when it is small at an early stage. The purpose of this work is to design a low-cost microstrip patch antenna sensor suitable for detecting brain cancer tumours. The computer simulation technology CST Studio Suite 3D EM simulation and analysis was used to create a patch antenna with different frequencies of 2.8 GHz, 3.9 GHz, 5 GHz, and 5.6 GHz to diagnose brain tumours. A comparison study between these resonance frequencies (lower-band (L-B) 2 GHz, middle-band (M-B) 3.9-5 GHz, and upper-band (U-B) > 5 GHz) has been performed using a six-layer brain phantom consisting of fat, dura, brain, skin, CSF (Cerebrospinal Fluid), and skull. The designed patch sensor was assessed in both scenarios, with and without a tumour cell, on a brain phantom. Three parameters have been observed: the frequency phase shift, the depth of reflection return loss, and power absorption, which were used to indicate the presence of tumour cells. This study concludes that the middle-band (M-B) results in good penetration and a better return loss depth of around -20 dB. Meanwhile, the higher band provides a high resolution of 21 MHz phase shift, but with only a depth value of difference return loss of -0.1 dB. The proposed work could provide a pathway for designing patch sensors for biomedical applications.

Keywords: Antenna; Specific Absorption Rate; Brain Tumour; Phase Shift; Return Loss.

I. INTRODUCTION

Cancer is the most prevalent disease over the last five decades and can affect other standard body parts. Brain tumours, however, are one of the most dangerous diseases internationally, as they can affect different tissues in the human body. In the USA, in 2017, around 23,800 patients were diagnosed with brain tumours, and about 16,700 died in the same year [1]. The standard methods utilized to detect cancer are positron emission tomography (PET), X-ray screening, ultrasound imaging, computed tomography (CT) scan and magnetic resonance imaging (MRI) scanning [2]. Despite the variance of these techniques and their accuracy, most of them are complicated, expensive, and bulky.

One method of diagnosing brain cancer is ultrasound imaging; however, this method suffers from the quality of the images, which sometimes cannot be clearly distinguished between a healthy cell and a modified cell in its initial stage [3]. In addition, this method could cause the worsening of the patients' lives due to misdiagnoses and inaccurate results in the first check [4]. The most advanced technique for examining brain cancer is magnetic resonance imaging (MRI), which is one of the most sensitive techniques available for imaging dense tissues. Despite the sensitivity of MRI, it is costly and complicated. In addition, the tumour cannot be detected accurately by using this method, which may lead to a mismatch in the extraction or could cause other complications [5].

In previous techniques, there are still some limitations, such as localisation issues, inaccurate results, bulky equipment, and complicated and expensive techniques. Thus, a new method has been introduced to detect brain cancer, which utilises microwaves. This will allow a non-invasive test, low in cost, less time and accuracy [6]. Microwave technique is considered to be an active wave-based nonionizing electromagnetic and noninvasive wave which enters human tissues without initiating health risks [7]. The main principle of using microwave technology is based on the electrical properties between normal and cancerous tissues [8]. Radar-constructed technique is a desirable technique because it considers and focuses on the electrical properties of the tumour [9].

The antenna is the most significant element in determining the quality of brain tumour detection; therefore, appropriate antenna requirements should be considered. Such a system should cover several factors, including compactness, simplicity of combination, ease of geometric construction, enhanced bandwidth, tiny size, gain, and directivity [10]. All the constraints can be implemented by creating a microstrip-patch antenna with light mass, low profile, planar construction, and low production cost [11].

Early-stage detection can reduce the treatment phase and cost [12]. Therefore, early diagnosis can save lives and achieve a 97% survival rate [4]. However, conventional microstrip patch antenna design requires adaptations for reliable wave transmission and reflected signal collection for brain malignant tumour detection. Thus, the goal of this research is to: (1) design confirmation of a low-cost and reliable microstrip patch antenna and (2) detect a tumour cell within the brain. In this approach, the design is presented numerically as a new microstrip patch antenna specifically designed for the detection of brain cancer. The structural design provides a consistent and competent way to identify brain tumours at an early stage. This study could be useful for biomedical applications.

Manuscript received on 24 January 2024 | Revised Manuscript received on 30 January 2024 | Manuscript Accepted on 15 February 2024 | Manuscript published on 28 February 2024.

*Correspondence Author(s)

Abdullah Alzahrani*, School of Electrical and Electronic Engineering, Taif University, Al Hawiyah, E-mail: aatyah@tu.edu.sa, ennnnng@gmail.com, ORCID ID: 0000-0002-2490-1466

© The Authors. Published by Blue Eyes Intelligence Engineering and Sciences Publication (BEIESP). This is an open access article under the CC-BY-NC-ND license <http://creativecommons.org/licenses/by-nc-nd/4.0/>

II. METHOD

The basic principle of this work is to design a microstrip patch antenna for observing reflected signals and distinguishing between the different electrical properties of cells. Normal and cancerous cells can be distinguished, as they exhibit different electrical properties. The patch antenna is the most essential element that needs to be considered in the system.

The basic principle is that the antenna transmits a microwave electromagnetic signal to a specific part of the body. Some of the signal scatters back to the antenna, depending on the dielectric properties of the cell. According to studies [13], the dielectric property of a healthy cell is lesser than a cancerous cell. Thus, it can be easily distinguished by using a backscattered signal to indicate the presence of a cancerous cell. Furthermore, further data can be obtained from the scattered back signal, which is valuable evidence, such as the depth of return loss and phase shift, revealing the existence of a cancer cell.

The direction of the radiation pattern (directivity), gain, matching feed-in, resonance frequency, efficiency and specific absorption rate SAR radiation are crucial parameters for our design to detect brain cancer cells firmly. All these parameters are taken into account in the design of the antenna. In this model, we focus on the antenna design, head phantom modelling, and the tumour located inside the brain. The phase shift and SAR values of the human head model were taken into consideration.

A. Antenna Patch Section Formula

All the requirements for designing the patch antenna were considered, including small size, light weight, cost-effectiveness, and ease of microstrip configuration. The design utilises flame-retardant epoxy resin and glass fabric composite (FR4) as the substrate, with $\epsilon_r = 4.3$, a thickness of $h = 1.6$, and a loss tangent of 0.025. Additionally, a copper

ground layer is used, with a thickness of 0.035 mm. The line feed of the microstrip is built as a central feeding procedure to match 50Ω . The formula of the patch's dimension is given as [14]:

Length of patch:

$$L = \frac{1}{2f_r \sqrt{\epsilon_{reff} \sqrt{\mu_0 \epsilon_0}}} = -2\Delta L \tag{1}$$

Where h is substrate thickness:

$$\epsilon_{reff} = \frac{\epsilon_r + 1}{2} + \frac{\epsilon_r - 1}{2} \left[1 + 12 \frac{h}{w} \right]^{-1/2} \tag{2}$$

$$\frac{\Delta L}{h} = 0.412 \frac{(\epsilon_{reff} + 0.3) \left(\frac{w}{h} + 0.264 \right)}{(\epsilon_{reff} - 0.258) \left(\frac{w}{h} + 0.8 \right)} \tag{3}$$

Wide of patch (Wp):

$$w = \frac{1}{2f_r \sqrt{\mu_0 \epsilon_0}} \sqrt{\frac{2}{\epsilon_r + 1}} = \frac{v_0}{2f_r} \sqrt{\frac{2}{\epsilon_r + 1}} \tag{4}$$

where ϵ_r = dielectric constant of substrate
 ϵ_{reff} = Effective dielectric constant
 W_p = Width of the patch

B. Substrate and Ground Planes

Length of substrate plane (Ls):

$$L_s = 6h + L \tag{5}$$

Wide of substrate plane (Ws):

$$W_s = 6h + W \tag{6}$$

The ground width is identical to the substrate width.

C. Antenna Sensor Construct

The construction of the patch antenna sensor, along with its dimensions, is illustrated. Initially, a simple rectangular microstrip is designed with multiple slots and varying resonant frequencies. Additionally, a line feeding practice is employed to feed the antenna, and a 50Ω impedance match is achieved. The sizes and geometry of the antenna and ground structure are shown in Figure 1.

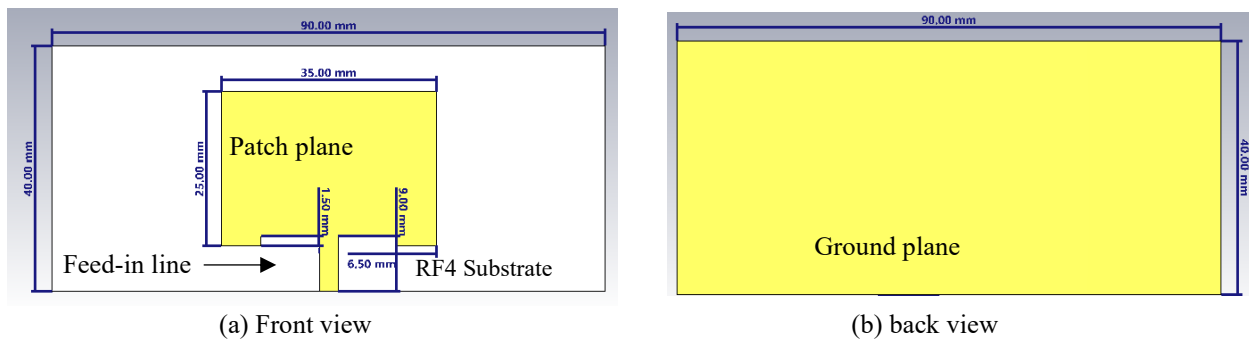


Figure 1. Structure of the Microstrip Patch Antenna, (A) Front Patch and (B) Back Patch

Figure 1 illustrates a microstrip patch antenna design comprising three layers: the background, the middle substrate, and the top patch. The dimensions of the antenna sensor (substrate) and patch are 40 mm × 90 mm and 35 mm × 25 mm, respectively. As shown in Figure 1, the background plane covers the entire backside of the antenna, utilising the same size substrate to enhance the antenna's efficiency. On the front side of the patch antenna, a slight cut-out on the rectangular patch from the bottom side has been considered, which can help enhance the bandwidth and alter the location of the resonance frequency. Furthermore, the antenna design

was constructed to work at different resonant frequencies, specifically 2.8 GHz, 3.9 GHz, 5 GHz, and 5.6 GHz. All optimisations and modifications to the design (e.g., introducing cut-outs, slots, grounds, sizes, and thickness) will enhance the efficiency of the antenna and emphasise return loss at the specific resonance frequency, taking into account all these factors.

D. Phantom Brain Model

According to a study [12] and its calculations, table 1

Published By:
 Blue Eyes Intelligence Engineering
 and Sciences Publication (BEIESP)
 © Copyright: All rights reserved.

shows the obtained material parameters (ϵ and σ) dielectric properties for the circular brain structure, which indicate that both the conductivity and permittivity for the different frequencies from 3 GHz to 8 GHz. The phantom brain model was designed using CST software.

Table 1: Dielectric Properties of Different Layers in Head Phantom

Tissue	Permittivity (ϵ)	Conductivity (σ)
Brain	43.22	1.29
CSF	70.1	2.3
Dura	46	0.9
Bone	5.6	0.03
Fat	5.54	0.04
Skin	45	0.73
Tumor	55	7

It can be seen from Figure 2 that the phantom head consists of six layers: outer Skin, Fat, Bone (skull), Dura, CSF, and Brain. Figure 2 illustrates the brain model.

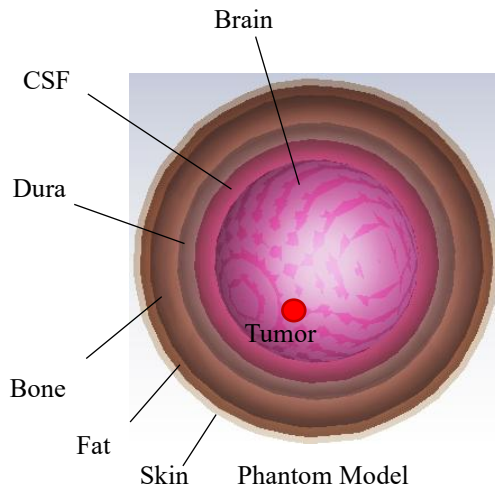


Figure 2. Phantom Head Model and Layers

III. RESULTS

A head model is constructed using the CST software to assess the entire system's action in detecting cancer cells, which is used as a realistic phantom. All dielectric properties, including conductivity and permittivity, were considered in

the different layers. The position of the patch antenna was continually changing to collect backscattering signals from various sides. In the results section, a comparison study is presented and discussed, utilising different resonance frequencies at 2.8 GHz, 3.9 GHz, 5 GHz, and 5.6 GHz, with and without cancer cells, as illustrated in Figure 3.

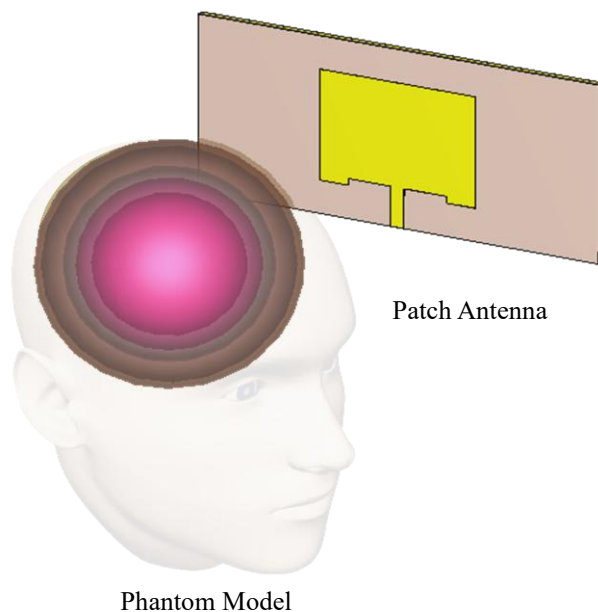


Figure 3. Antenna Patch Sensor with Phantom Brain Model

A Low-Cost Patch-Antenna for Non-Invasive Brain Cell Detection

A. Return Loss:

The first parameter considered and analysed is the return loss (S11) at the resonance frequencies of 2.8 GHz, 3.9 GHz, 5 GHz, and 5.6 GHz. Each reflectance value shown below is

below -10 dB, which complies with the criteria. Figure 4 shows the graphs of the return loss profile for the reflector (S11) antenna sensor for both normal brain (Figure 4a) and affected cancerous brain (Figure 4 b).

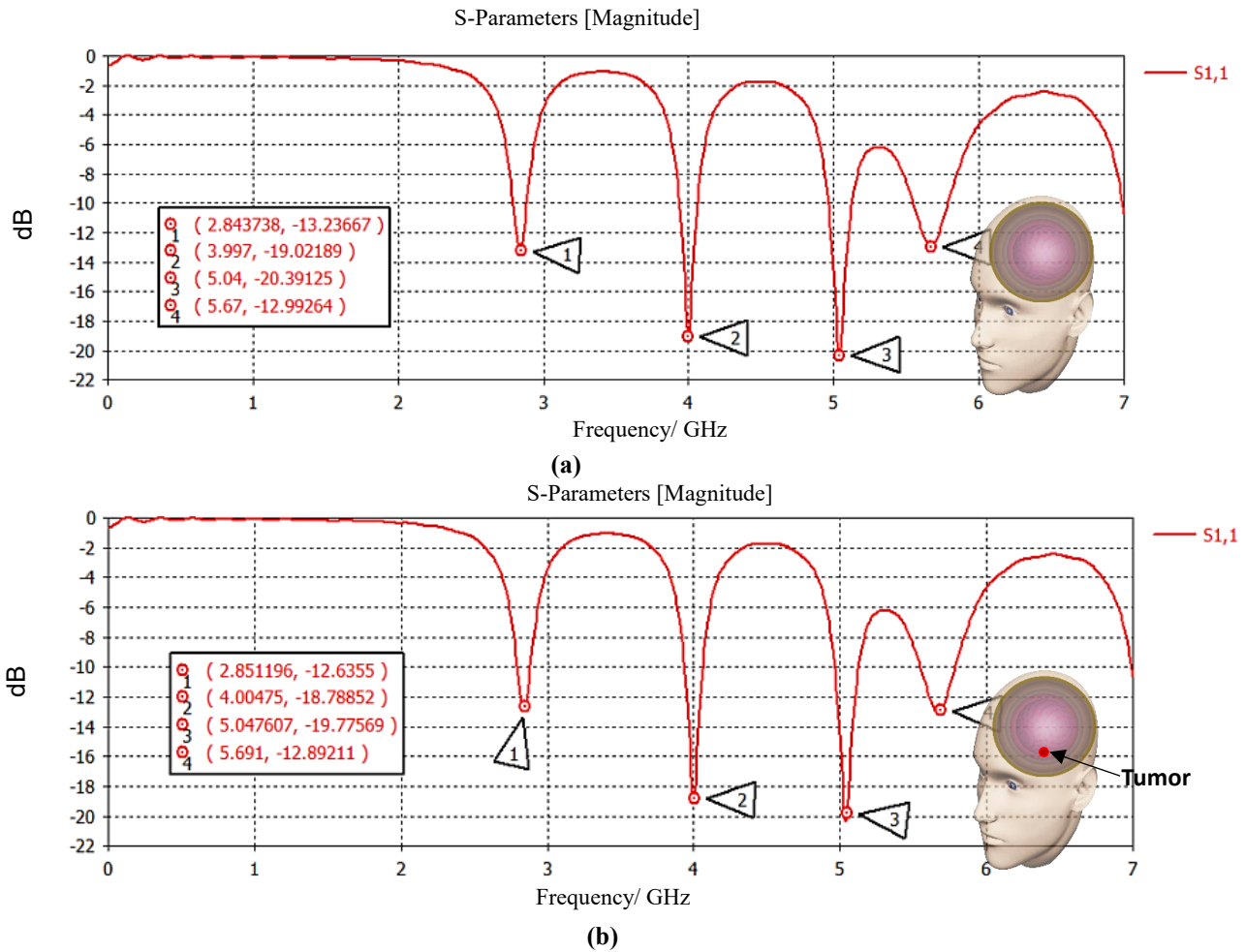


Figure 4. Return Loss Profile for Reflector (S11) Antenna Sensor, (A) without Tumor and (B) With Tumor Cell

As shown in Figure 4, at a resonance frequency of 2.8 GHz, the phase shift between the standard and affected cells is approximately 7.45 MHz. At a frequency of 3.9 GHz, the phase difference is approximately 7.75 MHz. At 5 GHz, the difference is 7.60 MHz, and at the higher frequency of 5.6

GHz, the phase difference is around 21 GHz. Table 2 summarises the depth value of return loss (S11) at each resonance frequency and the corresponding phase difference/depth value with and without tumour cells.

Table 2: Resonance Frequencies and Difference Values Without/With Tumour Cell

Without Tumour Cell		With Tumour Cell		Phase Difference		Depth Value Difference	
Frequency (GHz)	S11 (dB)	Frequency (GHz)	S11 (dB)	Frequency (MHz)	S11 (dB)	S11 (dB)	S11 (dB)
2.843738	-13.23667	2.851196	-12.6355	7.458	-12.6355	-13.23667	-0.60
3.997	-19.02189	4.00475	-18.7885	7.75	-18.7885	-19.02189	-0.23
5.04	-20.39125	5.047607	-19.7757	7.607	-19.7757	-20.39125	-0.62
5.67	-12.99264	5.691	-12.8921	21.0	-12.8921	-12.99264	-0.10

B. The Voltage Standing Wave Ratio (VSWR)

The VSWR is one of the parameters used in the design to indicate the mismatch between the feed line connecting to the

antenna patch. The minimum level in the allowable range (i.e., below 2) can be achieved in our design. The results of the antenna design show the value of VSWR at the resonance frequencies, as shown in Figure 5.

Voltage Standing Wave Ratio (VSWR)

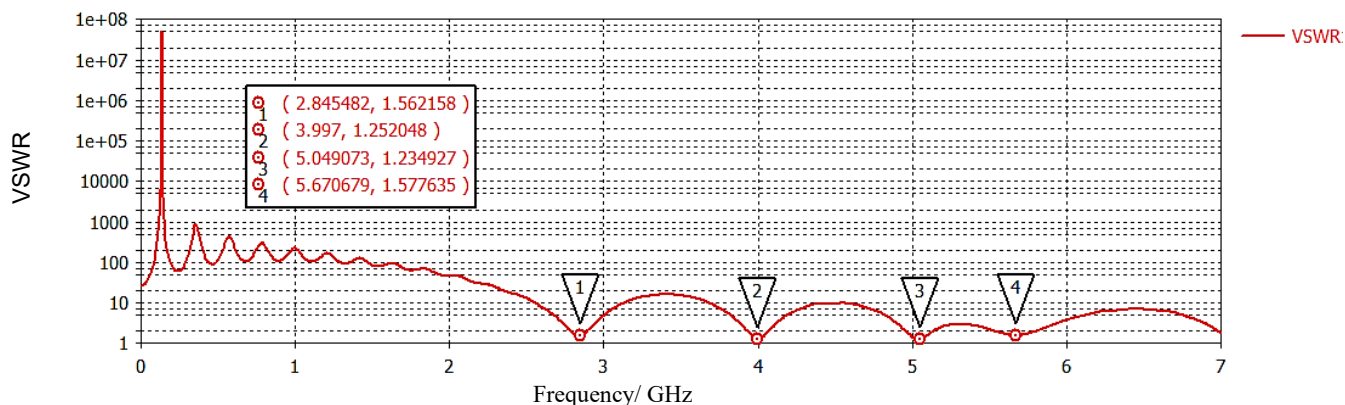
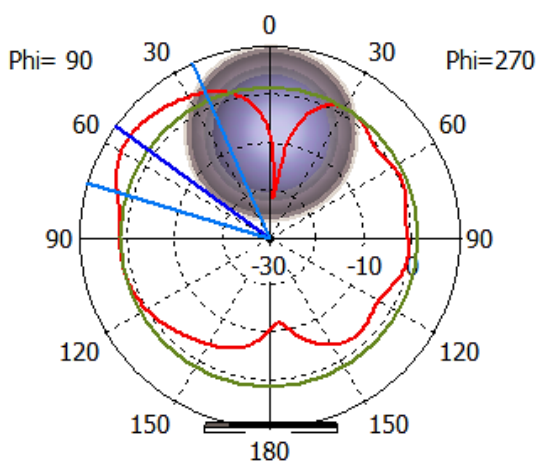


Figure 5. The Voltage Standing Wave Ratio (VSWR)

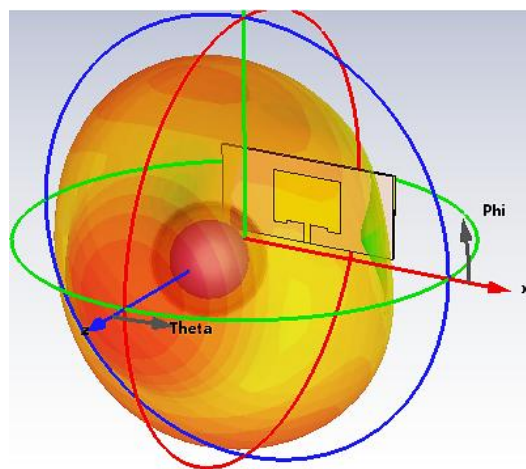
At the resonance frequencies of 2.84, 3.99, 5.04, and 5.67 GHz, the VSWR values are 1.56, 1.25, 1.23, and 1.57, respectively. All VSWR values are under two, which is suitable for the application. Thus, the antenna design is described as having a “Good Match”, and when the value of VSWR exceeds 2 for a frequency of interest, it means that the design of the antenna is poorly matched. In our design, all values of VSWR are less than < 2 , which indicates that the values are in the acceptable range and a great match.

C. Radiation Pattern

The theta and phi components refer to basic measurements in a spherical coordinate system. The spherical coordinates relate to the Cartesian axes: Theta = 0 for 360 and Phi = 0 for x-z Cut, Phi = 90 for y-z Cut. The x-z plane ($\phi = 0$) is referred to as the E-plane (x-z plane), whereas the y-z plane ($\phi = 90$) is referred to as the H-plane, respectively. The radiation pattern of the proposed antenna in the H-plane (y-z plane) is shown in Figure 6 (a) and (b), and the 3-dimensional radiation pattern is shown in Figure 6 (b). The beams in E-plane and H-plane are favourable because the primary lobes' orientation is stable with broadside beams.



(a) 2-D radiation



(b) 3-D far-filed

Figure 6. Radiation Pattern of the Patch Antenna in H-Plane (Y-Z Plane) and E-Plane (X-Z Plane)

From figure 6 (a), the main lobe magnitude = 6.22 dBi, the main lobe direction = 54.0 deg. And the angular width (3dB) = 49.3 degrees. The simulated gain and directivity are plotted and calculated for all resonance frequencies. The observed gain and directivity of each resonance frequency are summarised in Table 3.

Table 3: Gain and Directivity at Resonance Frequencies

Frequency (GHz)	Gain (dBi)	Directivity (dBi)
2.84	2.72	7.34
5.04	0.30	6.61
5.68	3.75	8.12

D. Specific Absorption Rate (SAR)

One of the critical parameters is the SAR absorption rate of radiation. To avoid health risk, the specific absorption rate (SAR) must not exceed 2 Watts per kilogram. The International Commission on Non-Ionising Radiation Protection (ICNIRP) has recommended the SAR limit since 1998.

The SAR is obtained by dividing the total power absorbed in the human body by the full body weight. A local SAR is calculated and expressed as a numerical value per volume

element, forming a space distribution function. The Telecommunication Technology Council Agenda No. 89 and CENELEC 1995 specify typical SAR values averaged in tissue masses of approximately 10g. In contrast, the value of 1g is adopted by ANSI/IEEE C95.1-1992 of the United States. A cuboid averaging volume is used. Thus, in this work, the masses of 10g and 1g have been calculated, with the maximum SAR values of 1.3 W/kg for 10g and 2.1 W/kg for 1g, respectively.

IV. DISCUSSION

The antenna design was modelled and simulated using CST Studio; the design was completed, featuring layers of antenna with a full ground plane and a patch with no slot. By utilising the full ground plane, the return loss was excellent, with values less than -10 dB for all resonance frequencies. On the other hand, the SAR radiation was at a borderline value of 2.1 W/kg at 1g maximum SAR. For the 10 grams of tissue, the maximum SAR of 1.3 W/kg is in the acceptable range, less than < 1.6 w/kg. The SAR, in simple terms, refers to the rate at which the body absorbs RF energy. Therefore, the antenna design presented in this work is well-suited for biomedical applications.

Although the phase difference at the upper-band frequency of 5.67 GHz is 21 MHz, the depth value difference is worse, at around -0.10 dB. The resolution of the middle-band frequency, 3.99 and 5 GHz, is significantly better in terms of return loss, at -18.78 and -19.77 dB, respectively. However, the phase difference in the middle band is approximately 14 MHz less than that found in the upper band. In addition, the depth value difference of the return loss in the middle band is notable and could be used as a reliable indicator of tumour cells present. At a lower-band frequency of 2.84 GHz, the depth difference between the two measurements (without and with tumour cells) is -0.60 dB.

Additionally, the resonance frequency was approximately 6 GHz, which is distant from the lower band frequency and is not suitable for deep penetration. Then, the antenna was enhanced by introducing a cut around the two-edge bottom side of the patch antenna, with a width of 1.5 mm and a length of 6.5 mm. The resonance frequency shifts to a lower band frequency around 3 GHz, and we obtained four resonance frequencies at 2.8 GHz, 3.9 GHz, 5 GHz, and 5.6 GHz.

Accepted power and absorbed power: In both instances (without/with tumour), the stimulated power remained constant at 0.5 W. However, there were slight disparities in the accepted power: 0.476622 W for the non-tumour phantom and 0.47487 W for the tumour phantom. This suggests that the tumour's presence causes a slight modification in the way the tissue absorbs energy. In the tumour case, the absorbed power was marginally higher at 0.273287 W, compared to the non-tumour case, which had an absorbed power of 0.271856 W. The total Specific Absorption Rate (SAR) in the tumour phantom was 0.42595 W/kg, which was lower than the SAR in the non-tumour phantom, which was 0.437733 W/kg. Indications suggest that the tumour affects the dispersion of absorbed energy. Furthermore, the maximum specific absorption rate (SAR) was significantly lower in the tumour scenario compared to the non-tumour scenario. This distinction is crucial, as it emphasises how the presence of a

tumour can affect the specific points of absorption within the tissue. The highest specific absorption rate (SAR) measured over 10 grams of tissue was lower in the tumour scenario (1.39596 W/kg) compared to the non-tumour scenario (1.64121 W/kg). The maximum SAR point's coordinates experienced a slight shift, indicating a modification in the local energy absorption pattern due to the tumour's presence.

A higher penetration depth can be achieved with a lower frequency and lower resolution. Meanwhile, a better resolution can be achieved with a higher frequency; however, the penetration depth will be reduced, as seen in the comparison study in Table 2. The low-frequency band offers deeper penetration (lower loss), although the higher-frequency band provides a better resolution range in terms of phase shift, but offers less depth value difference. Hence, the choice of a middle band as an appropriate operating frequency ensures internal views of normal and tumour brain with good depth penetration and high resolution. In brief, a higher band (upper band) frequency provides resolution but with less penetration, and could miss the tumour cell if it is located deeper. Thus, middle-band frequency is preferable, as shown in the results. More than one antenna patch sensor can be mounted around the head to overcome the penetration issue and improve the localisation of the tumour cell. In the case of one patch antenna sensor that is far away from the tumour, the other one could be closer and can detect it easily. The difference is attributed to the return loss and its depth value, as well as the frequency phase shift measurements, due to the absence (in the normal cell) and presence of tumour cells. Moreover, the SAR analysis reveals significant disparities in the way energy is absorbed and distributed between cases with tumours and those without tumours. These results are acceptable and warrant further investigation into their practical application.

V. CONCLUSION

A new patch antenna was designed for brain tumour detection at multiple resonance frequencies of 2.8 GHz, 3.9 GHz, 5 GHz, and 5.6 GHz. The CST Study was used to model and simulate both the antenna and the phantom head. The realised gain of the antenna design at the resonance frequencies (return losses at the middle-band frequency) was -19 dB, while at higher or upper band frequencies, it is around -12 dB. It was also observed from the work that, although the higher band frequency has a lower return loss depth than the middle band frequency, it provides identifiable detection and higher resolution (recognisable phase shift value), which is better than the lower band frequency. A comparison study of antenna performance at different resonance frequencies was conducted. The phantom model was studied and evaluated with and without tumour cells, showing the validation of the approach. Critical parameters, such as gain, directivity, VSWR, impedance matching, and SAR, were considered in the patch antenna design, and all values are recommended and meet the requirements and standards of relevant organisations.



The proposed design is a harmless device for biomedical applications, specifically for detecting brain tumours.

ACKNOWLEDGMENTS

The author acknowledges and would like to thank the Ministry of Higher Education in the Kingdom of Saudi Arabia, represented at Taif University, Taif, Saudi Arabia.

DECLARATION STATEMENT

Funding	No, I did not receive.
Conflicts of Interest	No conflicts of interest to the best of our knowledge.
Ethical Approval and Consent to Participate	No, the article does not require ethical approval or consent to participate, as it presents evidence that is not subject to interpretation.
Availability of Data and Material/ Data Access Statement	Not relevant.
Authors Contributions	I am the sole author of this article.

REFERENCES

- R. L. Siegel, K. D. Miller, and A. Jemal, "Cancer statistics, 2017," *CA: A Cancer Journal for Clinicians*, vol. 67, no. 1, pp. 7–30, 2017. <https://doi.org/10.3322/caac.21387>
- B. J. Mohammed, A. M. Abbosh, S. Mustafa, and D. Ireland, "Microwave system for head imaging," *IEEE Transactions on Instrumentation and Measurement*, vol. 63, no. 1, pp. 117–123, 2014. <https://doi.org/10.1109/TIM.2013.2277562>
- A. Hossain, M.T. Islam, M.E.H. Chowdhury, H. Rmili and M. A Samsuzzaman "Planar Ultrawideband Patch Antenna Array for Microwave Breast Tumor Detection". *Materials* 2020, 13, 4918. [PubMed]. <https://doi.org/10.3390/ma13214918>
- M.A.Aldhaebi, K. Alzoubi, T.S. Almoneef, S.M. Bamatraf, H. Attia and O.M. Ramahi "Review of Microwaves Techniques for Breast Cancer Detection". *Sensors* 2020, 20, 2390. <https://doi.org/10.3390/s20082390>
- M.Z. Mahmud, M.T. Islam, N. Misran, S. Kibria, and M.Samsuzzaman, "Microwave Imaging for Breast Tumour Detection Using Uniplanar AMC Based CPW-Fed Microstrip Antenna". *IEEE Access* 2018, 6, 44763–44775. <https://doi.org/10.1109/ACCESS.2018.2859434>
- M. Ostadrahimi, P. Mojabi, S. Noghianian, L. Shafai, S. Pistorius, and J. Lovetri, "A novel microwave tomography system based on the scattering probe technique," *IEEE Transactions on Instrumentation and Measurement*, vol. 61, no. 2, pp. 379–390, 2012. <https://doi.org/10.1109/TIM.2011.2161931>
- F. S. G. B. Barnes, *Handbook of Biological Effects of Electromagnetic Fields*, CRC/Taylor & Francis, Boca Raton, FL, USA, 2007
- N. K. Nikolova, "Microwave imaging for breast cancer," *IEEE Microwave Magazine*, vol. 12, no. 7, pp. 78–94, 2011. <https://doi.org/10.1109/MMM.2011.942702>
- A. E. Souvorov, A. E. Bulyshev, S. Y. Semenov, R. H. Svenson, and G. P. Tasis, "Two-dimensional computer analysis of a microwave fat antenna array for breast cancer tomography," *IEEE Transactions on Microwave Theory and Techniques*, vol. 48, no. 8, pp. 1413–1415, 2000. <https://doi.org/10.1109/22.859490>
- M. Rokunuzzaman, M. Samsuzzaman, and M. T. Islam, "Unidirectional Wideband 3-D Antenna for Human Head-Imaging Application," *IEEE Antennas and Wireless Propagation Letters*, vol. 16, pp. 169–172, 2017. <https://doi.org/10.1109/LAWP.2016.2565610>
- I. Singh and V. S. Tripathi, "Microstrip patch antenna and its applications: a survey," *International Journal of Computer Applications in Technology*, vol. 2, no. 5, pp. 1595–1599, 2011. <https://doi.org/10.14569/IJACSA.2011.020319>
- R. Inum, Md. Masud Rana, K. N. Shushama, and Md. A. Quader, "EBG-Based Microstrip Patch Antenna for Brain Tumour Detection via Scattering Parameters in Microwave Imaging System," *International Journal of Biomedical Imaging*, Volume 2018, Article ID 8241438, 12 pages. <https://doi.org/10.1155/2018/8241438>
- M. Hussein, F. Awwad, D. Jithin, H. Hasasna, K. Athamneh and R. Iratni, "Breast cancer cells exhibit specific dielectric signature in vitro using the open-ended coaxial probe technique from 200 MHz to 13.6 GHz," *Sci. Rep.* 2019, 9, 4681. <https://doi.org/10.1038/s41598-019-41124-1>

- Balanis, Constantine A. *Antenna Theory: Analysis and Design*. 3rd ed. Hoboken, NJ: John Wiley, 2005

AUTHOR PROFILE



Abdullah Alzahrani, BSc, MSc, PhD, is an Assistant Professor at Taif University, Electrical and Electronic Department. He also worked for two years as a Research Associate in Electronic Smart Sensors at the Electrical Engineering, Cambridge Graphene Centre (CGC), The University of Cambridge, UK. Before joining the University, Alzahrani worked at different institutes (College of Technology (KSA) and Loughborough University (UK)), and he also worked at start-up companies (Cerebrum Matter LTD, UK) that specialised in EEG and Alzheimer's. The main areas he works with and focuses on are integrated smart sensors, Micro-devices, Biomedical wearable physiological sensors, environmental sensors, embedded systems, and electronic communication design. Alzahrani is a member of SPIE and IEEE, as well as a member of the reviewer board for the *Advanced Research in Electrical, Electronics, and Instrumentation Journal*. Alzahrani is a venture member at Haydn Green Institute for Innovation and Entrepreneurship, the University of Nottingham, UK. Intellectual property (IP) related to magnetoresistive technology has been filed with Cambridge Enterprise, the University of Cambridge, UK.

Disclaimer/Publisher's Note: The statements, opinions and data contained in all publications are solely those of the individual author(s) and contributor(s) and not of the Blue Eyes Intelligence Engineering and Sciences Publication (BEIESP)/ journal and/or the editor(s). The Blue Eyes Intelligence Engineering and Sciences Publication (BEIESP) and/or the editor(s) disclaim responsibility for any injury to people or property resulting from any ideas, methods, instructions or products referred to in the content.